One- and Two-Color Photon Echo Peak Shift Studies of Photosystem I

Harsha M. Vaswani,[†] Jens Stenger,[†] Petra Fromme,[‡] and Graham R. Fleming*[,†]

Department of Chemistry, University of California at Berkeley and Physical Biosciences Division, Lawrence Berkeley National Laboratory, Berkeley, California 94720, Department of Chemistry and Biochemistry, Arizona State University, Tempe, Arizona 85287-1604

Received: February 16, 2006; In Final Form: September 12, 2006

Wavelength-dependent one- and two-color photon echo peak shift spectroscopy was performed on the chlorophyll Q_y band of trimeric photosystem I from *Thermosynechococcus elongatus*. Sub-100 fs energy transfer steps were observed in addition to longer time scales previously measured by others. In the main PSI absorption peak (675−700 nm), the peak shift decays more slowly with increasing wavelength, implying that energy transfer between pigments of similar excitation energy is slower for pigments with lower site energies. In the far-red region (715 nm), the decay of the peak shift is more rapid and is complete by 1 ps, a consequence of the strong electron−phonon coupling present in this spectral region. Two-color photon echo peak shift data show strong excitonic coupling between pigments absorbing at 675 nm and those absorbing at 700 nm. The one- and two-color peak shifts were simulated using the previously developed energy transfer model (*J. Phys. Chem. B* **2002**, *106*, 10251; *Biophysical Journal* **2003**, *85*, 140). The simulations agree well with the experimental data. Two-color photon echo peak shift is shown to be far more sensitive to variations in the molecular Hamiltonian than one-color photon echo peak shift spectroscopy.

Introduction

The 96 nonequivalent chlorophylls (Chls) that constitute photosystem I (PSI)[1] make understanding the design mechanism and determining the energy transfer pathways challenging. As in the purple bacterial system, the distribution of site energies (energetic disorder) plays a key role in funneling the energy efficiently to the reaction center (RC). In PSI, energetic disorder is intrinsic, caused by the seemingly haphazard arrangement of the Chls and their individual interactions with various amino acid side chains and water molecules.[2,3] The density of the pigments may allow for many different pathways of energy flow from any given Chl molecule, further complicating the problem.

Many studies have focused on whether PSI is transfer-to-trap limited or trap-limited by determining the energy transfer steps within PSI.[4−16] Previous time-resolved fluorescence experiments on PSI from *Thermosynechococcus elongatus* have revealed several femtosecond and picosecond time scales of energy transfer: 360 fs, 3.6 ps, 9.8 ps, and 38 ps.[9,17] These time scales have been attributed to various Chl−Chl energy transfer steps involving energy equilibration within the main absorption peak (360 fs) and energy transfer from the bulk Chls (absorbing at 665−690 nm) to those absorbing at 710 nm (3.6 ps) and to the Chls absorbing even lower wavelengths of light (9.8 ps).[9,17] The 38 ps component is responsible for the largely wavelength-independent trapping time and corresponds to the time in which excitations are captured by P700. Additional time scales have been observed by Gobets et al. corresponding to an uphill energy transfer from pigments absorbing at 700 nm (700 fs) and 710 nm (1.6 ps) to those absorbing in the main absorption peak.[17] Melkozernov et al. measured a similar time scale of 1.5−2.5 ps in PSI from *Synechocystis* sp. PCC 6803 corresponding to both uphill and downhill energy transfers between pigments absorbing at 685 nm and those absorbing around 710 nm.[10] At 77 K, an uphill energy transfer from 712 nm to the bulk Chl region can be as fast as 160 fs.[11]

While these population sensitive techniques have helped us understand energy flow between different spectral regions, a true understanding of energy flow in PSI requires connection of the spatial and energetic dynamics, along with the individual microscopic time scales of energy transfer. The rise and decay of a single energy transfer step typically cancel in pump−probe experiments. There have been numerous speculations of the time scales of "energy equilibration",[6,8−10] the energy transfer times between isoenergetic pigments that are scattered throughout the antenna. Only a few experiments can probe this process. Transient absorption anisotropy experiments were performed on trimeric PSI from *Synechocystis* sp. PCC 6803 at 680 and 710 nm, revealing decay kinetics of 590 fs and ∼3.1 ps, respectively.[8] Fluorescence anisotropy measurements on PSI from *Thermosynechococcus elongatus* revealed time scales of ∼100 fs and ∼1.6 ps using excitation and detection wavelengths of 650 and 725 nm, respectively,[9] but fluorescence anisotropy experiments are limited to detecting fluorescence spectrally distant from the excitation wavelength and have lower time-resolution than other femtosecond techniques.

Many theoretical studies, prompted by the first high-resolution X-ray structure (2.5 Å) of PSI,[1] have attempted to provide a microscopic description of energy transfer in PSI by modeling the spectroscopic characteristics of individual Chl molecules, Chl−Chl interaction, and excitation energy flow within the antenna.[18−23] Byrdin and co-workers used Förster and excitonic coupling theory to study the relationship between structure and function.[18] Their spectral assignments of Chl molecules and modeling of experimental linear and nonlinear spectra allow for speculation about the role of specific Chls, disorder, and pigment orientation in the energy transfer process and trapping.

* To whom correspondence should be addressed. E-mail: grfleming@lbl.gov.
† University of California at Berkeley.
‡ Arizona State University.

10.1021/jp061008j CCC: $33.50
Published on Web 11/23/2006

Sener et al. developed the sojourn expansion (within master equation calculations) to model the energy transfer dynamics of PSI and, in particular, capture repeated trapping and detrapping events.[20] They investigate the efficiency of monomeric and trimeric PSI and the role of key Chls by blocking particular energy transfer pathways either by omitting certain Chls or varying Chl orientation.[20,21]

A parallel approach has been used by our group. Previously we constructed the effective Hamiltonian of PSI by using the high-resolution crystal structure and the INDO/S method.[19] We calculated the Chl excitation energies and the Chl−Chl coupling strengths explicitly, including the effects of the protein environment on the site energies. The solution to the Hamiltonian matched the low-temperature experimental absorption spectrum. We then used the effective Hamiltonian to model energy transfer and trapping kinetics using modified Redfield/Förster theory, which interpolates between the strong and the weak coupling limit.[22,23] This novel approach was necessary to correctly take into account the wide range of coupling strengths in PSI. Master equation calculations successfully describe the experimental time- and wavelength-resolved fluorescence decays, provide justification for fitting the exponential decay curves with comparatively small numbers of exponential time constants, and give insight into the role of special Chls, namely, the linker Chls, the RC, and the red Chls, which absorb at longer wavelength with respect to the primary electron donor P700 at 700 nm. Further quantitative analysis of the energy migration and the dominant transfer steps resulted in the construction of kinetic domains that provide a coarse-grained picture of the dominant contributions to the overall trapping time scale.[22]

Even though the recent theoretical approaches are in good agreement with the available experimental spectroscopic data, many aspects of the model remain experimentally underdetermined. Linear spectra and population sensitive techniques do not probe the full Hamiltonian; in a system as spectrally congested as PSI, unambiguous information is difficult to obtain. The excitation energy and the coupling parameters of the Chl molecules cannot be extracted independently by these means, and the dynamics of energy transfer between isoenergetic pigments is not easily accessed.

Photon echo spectroscopy has the potential to overcome these shortcomings. Three-pulse photon echo peak shift (3PEPS) spectroscopy is a four-wave mixing technique sensitive to energy transfer, especially when the involved chromophores have similar transition energies.[24,25] 3PEPS allows us to follow the decay of phase memory and can distinguish between different levels of disorder and energy transfer.[24,26] For example, 3PEPS revealed the time scales between and within the photosynthetic rings of purple bacterial systems.[26−29] It has previously been shown that the peak shift is directly related to the transition energy fluctuation correlation function, $M(T)$, where T is the time delay between the second and third pulses.[30] Thus, the peak shift enables us to track the (transition frequency) memory of the system.[30]

Traditional 3PEPS is performed with three identical laser pulses and accesses the disorder and characteristics of the diagonal elements of the Hamiltonian. Two-color 3PEPS (2C3PEPS) has recently been developed[26,31,32] as a way to measure the off-diagonal elements, the electronic coupling terms.[25,33] In addition, 2C3PEPS is sensitive to pathways of energy flow through a quantity, the difference peak shift (DPS)[34] that is related to the conditional probability of the system interacting with light at frequency ω_2 at time T, given that the system was initially excited with frequency ω_1 at $T = 0$ (i.e., $P(\omega_2; T|\omega_1)$. In 2C3PEPS, the third pulse has different spectral properties from the first two pulses and can be thought of as a probe pulse. 2C3PEPS is a complementary technique to the recently developed heterodyne-detected 2D electronic spectroscopic method. While the coupling terms probed with 2D electronic spectroscopy are very sensitive to the transition dipole moment directions of the pigments, Cho et al. showed that the two-color peak shift is directly related to the *spatial* overlap of excitons absorbing at different frequencies.[35] 2C3PEPS is able to measure coupling between pigments that absorb in spectrally distant regions. Here, we extend the use of 2C3PEPS to an energy transfer system.

We present one-color (1C) and two-color (2C) 3PEPS measurements on PSI. 1C3PEPS data were obtained at four different spectral positions and two different spectral bandwidths within the Q_y absorption band of Chl in PSI.

Methods

Wavelength-Dependent, One-Color, Three-Pulse Photon Echo Peak Shift. Excitation light, tunable through the Chl Q_y band, was generated by an optical parametric amplifier (Coherent 9450 OPA) pumped by a 250 kHz regenerative amplifier (Coherent RegA 9000) with a stretcher/compressor (Coherent 9150) and a Mira Seed Ti/Sapphire oscillator. The pulses from the OPA were tuned and compressed to generate transform-limited pulses centered at 676, 690, 700, and 715 nm, with pulse durations of 30−33 fs. Additional experiments were carried out at 675 and 690 nm after spectrally filtering the pulses to a fwhm of 8−9 nm, resulting in pulse durations of 70−72 fs.

One-color, three-pulse photon echo peak shift measurements were carried out as previously described.[36−38] In brief, the pulses from the OPA were split into three parts of parallel polarization and approximately equal intensity. The three beams with wave vectors $\mathbf{k_1}$, $\mathbf{k_2}$, and $\mathbf{k_3}$ were focused into the sample in the conventional triangular geometry, and the time-integrated photon echo intensity was simultaneously detected in the two-phase matched directions $\mathbf{k_3} \pm (\mathbf{k_1} - \mathbf{k_2})$ as a function of the time delay between the first two pulses (coherence time τ) and the time delay between the second and third pulses (population time T). The time delays are scanned using a symmetric sweep, and the peak shift profiles (in the τ domain) are fit to Gaussians. The peak shift is defined as half the coherence time delay between the peak intensity measured at $\mathbf{k_3} + (\mathbf{k_1} - \mathbf{k_2})$ and at $\mathbf{k_3} - (\mathbf{k_1} - \mathbf{k_2})$ at a given population time. To minimize scatter, one beam was chopped and the signals were recorded using slow photodiodes and lock-in amplification. To ensure proper alignment and correct timing, the experiment was tested with a laser dye (Oxazine 750 or Rhodamine 800) before each measurement on PSI. With the exception of the power-dependence study, the excitation pulses were attenuated to 2 nJ per beam and focused so that 83−88% of the pulse energy passed through a 75 μm pinhole at the sample position.

Two-Color Photon Echo Peak Shift Spectroscopy. Two-color photon echo peak shift measurements, as well as additional one-color photon echo experiments, were performed using a home-built 3 kHz repetition rate laser system. The output of a regenerative amplifier[39] was used to pump a two-pass noncollinear optical parametric amplifier (NOPA) using a 2 mm BBO crystal and a single-filament white light seed generated in a 3 mm sapphire crystal. The white light in the NOPA was spectrally filtered to a fwhm of 10 nm centered at 675 and 690 nm for the one-color measurements and to a fwhm of 50 nm centered at 695 nm for the two-color measurements. For the two-color measurements, the output pulses were further filtered in the echo

interferometer to generate pulses centered at 675 and 700 nm with 10−14 nm fwhm. Using a dual prism compressor, the pulses were compressed to pulse durations of 70 fs for the one-color measurements and ∼80 fs for the two-color experiments. The cross-correlation in the two-color experiment was also ∼80 fs. The excitation pulses were attenuated to less than 2 nJ per beam and focused so that 55% and 70% of the pulse energy passed through a 75 μm pinhole for the two-color and one-color measurements, respectively.

The two-color 3PEPS experiment was performed as previously described.[34] Two different delay-scanning methods (scan A and scan B) were used to obtain the type I (τ_I*) and type II (τ_{II}*) peak shifts, emphasizing the echo and free-induction decay response, respectively. The population time is defined as the time delay between the second and the third pulses for scan A and the time delay between the first and the third pulses for scan B. The population time is held constant, while the coherence time is scanned by sweeping $\mathbf{k_1}$ and $\mathbf{k_2}$ for scan A and B, respectively. Instead of adding an additional translation stage to the setup for scan B, we scan through $\mathbf{k_2}$ by simultaneously scanning $\mathbf{k_1}$ and $\mathbf{k_3}$ across $\mathbf{k_2}$. The signal detected at $\mathbf{k_3} - (\mathbf{k_1} - \mathbf{k_2})$ is, therefore, the type I peak shift for scan A and the type II peak shift in scan B. Symmetrically, the signal detected at $\mathbf{k_3} + (\mathbf{k_1} - \mathbf{k_2})$ is the type II peak shift in scan A and the type I peak shift in scan B. The type I and type II peak shifts are then obtained by averaging the results of the two scans, in this way, accounting for any fluctuations or systematic errors in the zero coherence time. It is useful to define an additional quantity, the DPS, defined as DPS = type I − type II. The DPS measures the rephasing capability of the system and decays to zero when there is complete memory loss.

Sample Preparation. Trimeric PSI from the cyanobacterium *Thermosynechococcus elongatus* was prepared and crystallized as previously described.[2] All samples are prepared from freshly dissolved PSI crystals; the crystals were dissolved in a buffer containing 50 mM $MgSO_4$, 5 mM morpholine-ethanesulfonic acid (MES) pH 6.4, and 0.02% beta-dodecylmaltoside. The optical density of the sample in a 200 μm quartz cell was adjusted to 0.2−0.3 at the respective spectral positions within the absorption spectrum of PSI. Sodium ascorbate (10 mM) and 10 μM phenazine methosulfate (PMS) were then added to the samples to keep the RCs open for experiments conducted at 3 kHz. The measurements taken at a repetition rate of 250 kHz were done without addition of ascorbate and PMS so that P700 is oxidized ($P700^+$) and no electron transfer can occur (this is often called "closed RCs"). A peristaltic pump was used to flow the sample and to keep it at 5−6 °C by cooling the reservoir. To ensure sample stability, absorption and fluorescence spectra were taken before and after the measurements.

Theoretical Analysis. 3PEPS measures the memory of the system. We can model the data by computing the extent of correlation between the initial and the final states of the system and hence calculate the ability of the system to rephase. Faster energy transfer steps or weaker correlation between the initial and the final states results in more rapid decays of the peak shift. Conversely, stronger correlation or slower energy transfer dynamics results in higher peak shift values. In addition to sampling the inhomogeneous distribution, memory is also lost via "homogeneous" dephasing, that is, the fluctuations of the electronic transition frequency by the system phonons. If the peak shift decay is dominated by homogeneous dephasing from low frequency dissipative modes, then it is weakly sensitive to energy transfer. Fortunately, this is not the case in Chl−protein complexes in general and specifically in PSI. The PSI absorption spectrum is about three times wider than the Chla solution spectrum, even though the solution spectrum has greater reorganization energy. The low-frequency component of the reorganization energy is ∼165 cm^{-1},[40,41] leading to inhomogeneous broadening dominating the spectrum. In addition, our previous very detailed modeling of PSI[40] predicts many energy transfer rates (in the 96 × 96 rate matrix) corresponding to times of <100 fs, meaning that the sampling of inhomogeneous distribution will lead to substantial peak shift decay. We do not yet have a tractable approach to modeling the full one-and two-color peak shift data set that self-consistently allows for correlations between donors and acceptors, while fully incorporating the homogeneous dephasing. In this paper, we use two different approaches to calculate the rephasing capability of PSI. By comparing the two, we have confidence that our conclusions are robust and not excessively compromised by our model assumptions. First we assume that the inhomogeneous distribution of energy levels, rather than the homogeneous dynamics, produces the observed peak shift decay. We use the distribution of transition energies (taken from Damjanovic et al.[19]) to compute $I(T)$, the inhomogeneous contribution to the transition-frequency correlation function, $M(T)$. In this case, we neglect the contribution of rapid homogeneous energy fluctuations, a good approximation because Chl has a small Stokes shift, although the homogeneous broadening is properly included in the calculation of the energy transfer dynamics. Like the DPS, $I(T)$ is a time-correlation function that measures the fraction of the system that has rephasing capabilities and is related to the conditional probability of being at frequency ω_2 at time T, given that the system was initially excited with frequency ω_1 at $T = 0$, $P(\omega_2;T|\omega_1)$[22,34]

$$I(T) = \langle \delta\epsilon_{probe}(T)\delta\epsilon_{pump}\rangle_{inhom} = \frac{1}{N(T)} \equiv \int\int d\omega_1 d\omega_2 W(\omega_2|E_{pr})P(\omega_2;T|\omega_1)W(\omega_1|E_{pu}) \times \sigma_{abs}(\omega_1)[\omega_1 - \langle\omega\rangle_{pu}][\omega_2 - \langle\omega(T)\rangle_{pr}] \quad (1)$$

where $N(T)$ is the total population transferred from the pump to the probe region

$$N(T) \equiv \int\int d\omega_1 d\omega_2 W(\omega_2|E_{pr})P(\omega_2;T|\omega_1)W(\omega_1|E_{pu})\sigma_{abs}(\omega_1) \quad (2)$$

$W(\omega_1|E)$ is the probability of exciting a chromophore using the pump or probe pulse and σ_{abs} is the absorption cross-section for the transition energy in the equilibrium ground state. The $\langle\omega\rangle_{pu}$ and $\langle(T)\rangle_{pr}$ are the mean transition frequencies of PSI initially excited and probed at time T, respectively, and are given by

$$\langle\omega\rangle_{pu} = \frac{\int d\omega\ \omega\ W(\omega|E_{pu})\sigma_{abs}(\omega)}{\int d\omega\ W(\omega|E_{pu})\sigma_{abs}(\omega)}$$

$$\langle\omega(T)\rangle_{pr} = \frac{1}{N(T)}\int\int d\omega_1 d\omega_2 \omega_2 \times W(\omega_2|E_{pr})P(\omega_2;T|\omega_1)W(\omega_1|E_{pu})\sigma_{abs}(\omega_1) \quad (3)$$

In the case of one-color 3PEPS, $\omega_1 = \omega_2$. The conditional probabilities are computed from the population evolution of each exciton state calculated using the modified Redfield/Förster theory approach described by Yang et al.[40] The probabilities are weighted by the spectra of the first and third laser pulses

and then summed to give the total correlation between the initial and the final states. Static disorder is included explicitly by adding a random value selected from a Gaussian function with a width of 150 cm^{-1} to each of the site energies. The $I(T)$ is computed using the resulting Hamiltonians. This procedure is repeated for 20 samples to obtain the ensemble-averaged $I(T)$. While this method does not take into account pulse overlap effects, it does include experimentally determined spectral densities, the inhomogeneous Chl site energies and coupling strengths obtained in Damjanovic et al.,[19] and the full solution to the Pauli master equation. The resulting $I(T)$ values accurately describe the fluorescence and transient absorption time scales for the main Chl Q_y absorption band in PSI, suggesting that the intrinsic inhomogeneity of the site energies of Chls in PSI (and not the homogeneous energetic fluctuations) determines the energy relaxation pathways.

We can also calculate 3PEPS data by using the approach Yang and Fleming[24,25] developed for energy transfer systems. In this case, the rephasing and nonrephasing contributions to the signal are computed using a Gaussian distribution of Chl excitation energies with homogeneous and inhomogeneous widths equivalent to that of PSI (but not the exact site energies computed in Damjanovic et al.[19]). The total response function is obtained assuming

$$R(t,T,\tau) = R_{\text{echo}}(t,T,\tau)P_{\text{D}}(T) + R_{\text{FID}}(t,\tau)P_{\text{A}}(T) \qquad (4)$$

where R_{echo} is the response function of an isolated chromophore, and R_{FID} is the response function assuming no rephasing capabilities. P_{D} is the total population of Chls still at its initially excited site, and P_{A} is the total population of energy transferred to a different site. Equation 4 assumes transition frequency memory is lost after a single-energy transfer step. P_{D} and P_{A} are computed for a distribution of configurations from the master equation calculations, taking into account static disorder as well as the laser spectra of the first and third pulses. This approach includes pulse overlap effects and calculates the full response function using the bulk Chl spectral density, but averages over the site energies and energy transfer dynamics (and, therefore, the conditional probabilities) before the response functions are calculated. The master equation calculations are the same as those performed in Yang et al.,[40] with the following exception: the coupling (Huang−Rhys factor) to the 262 cm^{-1} mode in the line broadening function was changed from 0.1775 (obtained by Zucchelli et al.[42]) to 0.012 (obtained by Gillie et al.[41]), and the damping times of the 200−400 cm^{-1} modes were reduced from 1 to 0.5 ps. The peak shift was calculated using the line broadening function for bulk Chl. At 715 nm, the peak shift was also calculated using the line broadening function for Chls with charge transfer (CT) character and for P700 (with the same modifications to the modes as for the bulk Chls) to account for the stronger electron−phonon coupling (see Yang et al.[40])

Results and Discussion

One-Color Photon Echo Peak Shift Measurements. One-color photon echo measurements were performed at four different spectral positions and with two spectral widths within the absorption spectrum of PSI. The spectra of the laser pulses used and their position with respect to the PSI Q_y absorption band are illustrated in Figure 1. The spectra of the laser pulses are centered at 675, 690, 700, and 715 nm, probing Chls with an absorption around the band maximum as well as the red absorption tail that lies beyond P700.

The one-color peak shift measures time scales of energy transfer within the laser window. Figure 2a shows the temporal evolution of the peak shift recorded with three identical pulses (1C3PEPS) for the four different spectral positions. All traces start out at a peak shift of about 20−25 fs. This relatively large initial value compared to what is typically found with dye molecules in solution is similar to initial peak shift values seen in other light harvesting complexes such as light-harvesting complex II from plants[43] and purple bacterial light harvesting complexes[26−29] measured with laser pulses of similar temporal width. It hints to a relatively weak coupling of the excited Chl molecules to the protein bath because the initial peak shift is roughly inversely related to the mean square fluctuation amplitude of the transition frequency.

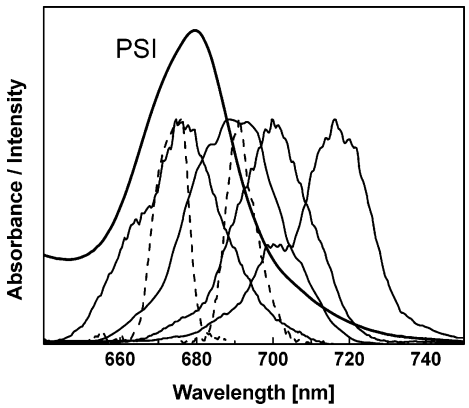

Figure 1. Absorption spectrum of the Q_y band of PSI (thick solid line) and the laser spectra of the pulses employed for the one-color photon echo experiments. The spectrally broad pulses with fwhm = 20−24 nm (thin solid lines) are centered at 676, 690, 700, and 715 nm, and the narrow bandwidth laser pulses with fwhm = 8−9 nm (dotted lines) are centered at 675 and 690 nm.

In contrast to the initial value, the decay of the PSI peak shift is very different for the four spectral positions. For laser pulses centered at 675, 690, and 700 nm, the decay becomes slower for increasing wavelength. At 700 nm, the peak shift does not decay at all within the detection window of up to T = 250 fs (Figure 2a). At 690 nm, the short component decays very rapidly (∼15 fs) but with a smaller amplitude. Most of the decay occurs on a time scale of 2−3 ps. Transient grating data (not shown)[44] show us that most of the Chls initially excited at 690 nm have transferred their excitation energy outside the detection window by 1−2 ps, therefore, the slower dynamics in the peak shift arise from only a small number of pigments. 1C3PEPS data captured at 675 nm can be described by a biexponential decay, with time constants of 90 fs (40%) and 1.5 ps (60%). The time scales of energy transfer observed here are substantially faster than the fastest energy transfer steps resolved previously.[8−10,17]

The peak shift behavior at 715 nm is strikingly different from the data obtained at spectral positions closer to the main absorption peak. The peak shift has decayed to half its initial value by 100 fs. A second decay component is found with a time scale on the order of about 800 fs. The decay of the peak shift suggests that all red Chls are completely dephased by 1 ps, whereas at shorter wavelengths, the finite long time peak shift indicates that a substantial inhomogeneity persists. Fluorescence anisotropy detected at 725 nm showed similar decay time scales to the peak shift of 95 ± 15 fs and 1.6 ± 0.14 ps.[9] This rapid decay most likely arises from strong electron−phonon coupling. The data support the notion (discussed in Damjanovic et al.[19] and Yang et al.[40]) that Chls absorbing in this region have strong electron−phonon coupling and/or exist as dimers, trimers, or even tetramers.

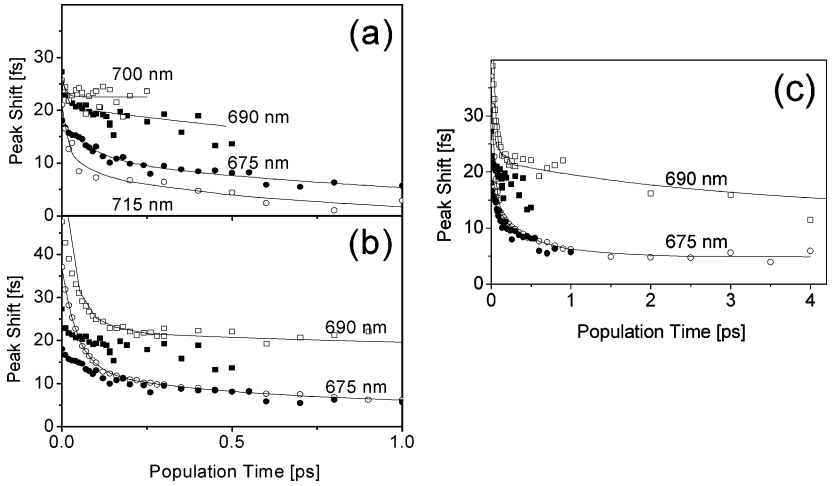

Figure 2. (a) One-color photon echo peak shift data measured at four spectral positions with fwhm = 20−24 nm (symbols). The solid lines represent a biexponential fit. (b,c) Narrow bandwidth (fwhm = 8−9 nm) peak shift data (open symbols) compared to the broad bandwidth data (solid symbols) taken with pulses centered at 675 and 690 nm. The solid lines represent biexponential fits to the narrow bandwidth data. Note the change in time scale between (b) and (c). For clarity, the biexponential fits to the broad bandwidth data are not shown in panels (b) and (c).

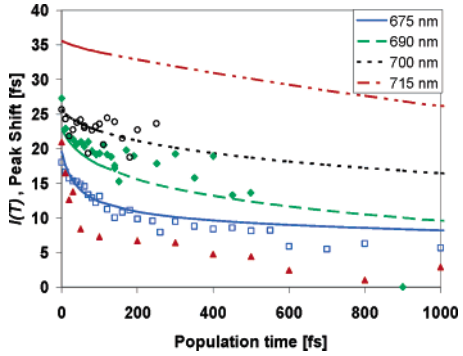

Figure 3. The calculated rephasing capability, $I(T)$, of PSI (lines) compared with the 3PEPS broad bandwidth measurements at 675 nm (squares), 690 nm (diamonds), 700 nm (circles), and 715 nm (triangles).

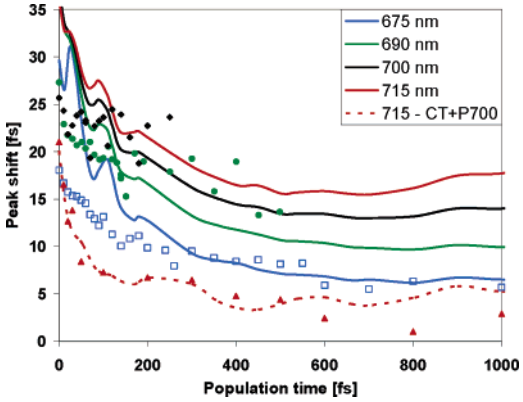

Figure 4. Simulated (solid lines) and observed (data markers) wavelength-dependent one-color photon echo peak shift data. The simulated peak shifts at 715 nm using the line broadening function for molecules with combined CT and P700 character is also shown.

Peak shift data taken with narrow bandwidth laser pulses are shown and compared to the broad bandwidth pulses in Figure 2b,c. The initial value of the peak shift, with all other parameters fixed, is directly proportional to the duration of the laser pulses. Thus, both narrow band experiments show significantly larger initial peak shift values. Apart from the pulse overlap effect, the behavior of the peak shift measured with laser pulses at 675 nm seems to be relatively insensitive to the bandwidth, suggesting homogeneous time scales of energy hopping around the main PSI absorption peak. At 690 nm, the peak shift in the narrow bandwidth measurement has a larger value even at longer times and a slower decay, suggesting slower energy transfer between pigments with site energies at 690 ± 5 nm compared to those absorbing at 690 ± 14 nm. The simplest picture consistent with this is that significant energy transfer must occur out of the 685−695 nm window but remain within the 676−704 nm region.

We can simulate the peak shift in two different ways as described in the theoretical methods section. The first is to compute the $I(T)$, the rephasing capability of the system taking into account only the inhomogeneous contributions to the peak shift, although both homogeneous and inhomogeneous broadening are properly included in the energy transfer calculation. The result is shown in Figure 3. We normalize the various $I(T)$s so that $I(0)$ computed at 700 nm matches the initial peak shift measured at 700 nm. The decay behavior of the 3PEPS data obtained at 675, 690, and 700 nm agree well with the simulated $I(T)$. However, our model predicts that the pigments absorbing at 715 nm should have a larger rephasing capability compared to the other wavelengths, whereas the opposite trend is observed in the experiment.

The peak shifts of PSI calculated by considering both the homogeneous and the inhomogeneous contributions (Figure 4) yield a similar trend to the $I(T)$: the computed peak shift curves are similar to those observed at 675, 690, and 700 nm, yet the model predicts slower dynamics between pigments at 715 nm than observed. The dynamics among pigments absorbing at 715 nm are clearly not well-reproduced by the model. As discussed in Yang et al.,[40] the pigments absorbing at ∼715 nm have strong electron−phonon coupling, and therefore, a different spectral density (and, consequently, a different line broadening function) is appropriate. The computed peak shift at 715 nm, using the average line broadening function for P700 and Chls with CT character is shown in Figure 4. The initial value of the peak shift at 715 nm, as well as its rapid decay, is well simulated using either the CT or the P700 line broadening function. The best fit to the experimental data is obtained by computing the peak shift, using the average of the CT and P700 line-broadening functions. The oscillations that appear in the calculated curves (but not in the experimental data) indicate that the coupling to a few of the modes in the bulk Chl line-broadening function is too strong. It is likely that further refinements of the spectral densities are necessary.

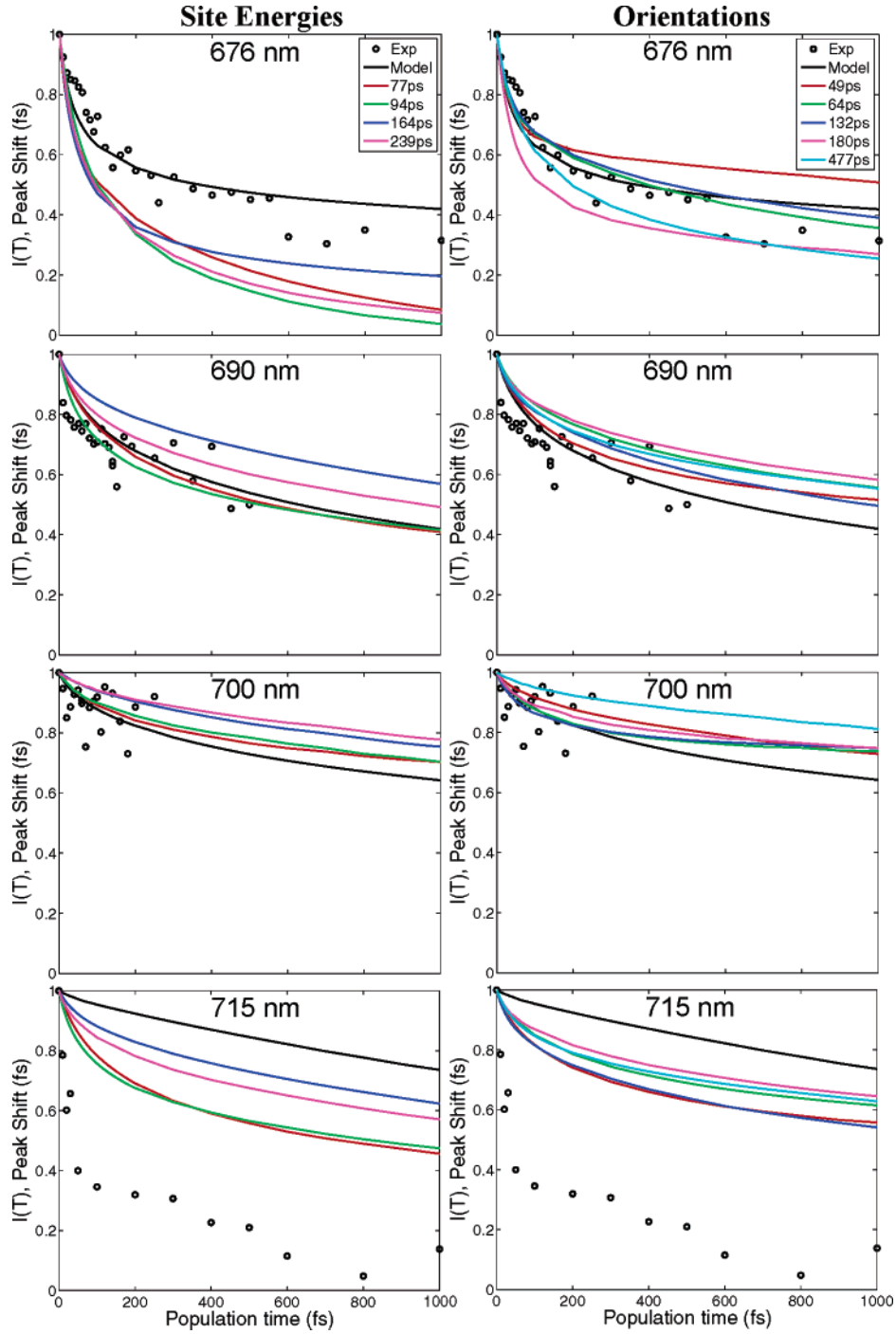

Figure 5. Calculated rephasing capability of PSI, $I(T)$, compared with the 1C3PEPS data ("x" markers). $I(T)$ is computed for permutations of the site energies (left) or orientations (right), holding the site energy/orientations of Chl EC-A1 (the epimer) constant, respectively. Trapping times for the permuted configurations are shown in the legend. The $I(T)$ for the model Hamiltonian calculated by Damjanovic et al.[19] (solid lines) is displayed.

Energy Landscape. A key motivation for carrying out experiments that are more complex to interpret than standard transient fluorescence and absorption studies is to test if the new methods are more sensitive to the microscopic details of the system than the standard techniques. For example, can the peak shift method distinguish between PSI models, where the same range of energies are present but are differently assigned to the individual Chl molecules? To explore this general topic, we tested the sensitivity of the rephasing capability of the system to the molecular Hamiltonian by computing $I(T)$ for a variety of modified Hamiltonians. We randomly shuffled the excitation energies or the orientations of all of the Chls except Chl EC-A1 (the Chl *a* epimer constitutes part of P700; nomenclature as per the protein data bank files[1−3]). Static disorder is included explicitly by adding a random value selected from a Gaussian function with a width of 150 cm^{-1} to each of the site energies, and the $I(T)$ is recomputed using the resulting Hamiltonians. This procedure is repeated for 20 samples over the inhomogeneous distribution to obtain the ensemble-averaged $I(T)$ for that Hamiltonian. When the site energies were shuffled, the coupling strengths were kept at the same values computed by Damjanovic et al.[19] When the orientations were shuffled, the site energies were held constant, but the coupling strengths had to be recalculated. Computing the full Coulombic coupling strengths of moderate to strongly coupling chromophores for all of the permutations would have been very computationally expensive,

therefore, for the latter calculations, we use the dipole approximation. As shown in Yang et al.,[22] the trapping times for these configurations have a narrow distribution when the energies or orientations of the RC and linker Chls are held constant and only the energies/orientations of the antenna Chls are randomly permuted. The absorption spectrum is also not sensitive to this type of variation. Figure 5 shows the normalized $I(T)$ computed for a few representative permuted Hamiltonians selected to have trapping times ranging from 49−477 ps and the original Hamiltonian (with trapping time 36 ps) constructed in Damjanovic et al.[19] were plotted with the 1C3PEPS data. The trapping time for the original Hamiltonian when only dipole−dipole couplings are included is 28 ps. The rephasing capability of the system is not strongly sensitive to variations in the site energies or pigment orientation. In fact, at 676 nm $I(T)$ decays more rapidly with the permuted site energies than both the 1C3PEPS data and the $I(T)$ computed using the calculated site energies from Damjanovic et al.,[19] implying that PSI is not optimized for rapid energy transfer between pigments absorbing at the peak of the Chl Q_y band. In all cases, the rephasing capability of the system decays more slowly with increasing wavelength. This can be explained by considering the number of pigments absorbing in each spectral region. Fewer Chls have site energies to the red of the absorption peak. If the site energies of the Chls are randomly distributed throughout the antenna, the average distance between the Chls absorbing at 700 nm is larger than between those absorbing at 690 nm, which in turn are larger than those between Chls absorbing at 675 nm. With larger interpigment distances, energy transfer rates between these Chls are slower, and the rephasing capability of the system within the bandwidth decays more slowly. In our model, this is also the case for pigments absorbing at 715 nm, and the $I(T)$ computed for the various Hamiltonians at 715 nm all decay very slowly compared to the experimental data. To explain the experimental data, the pigments absorbing at 715 nm must either be located far closer to each other than a random distribution would allow or, more likely, the Chls absorbing in this region have a much larger electron−phonon coupling, causing rapid dephasing.

The model captures the essence of the energy transfer dynamics within the Chl Q_y absorption band. The agreement between our experiment and the computed $I(T)$ and the relative insensitivity of the $I(T)$ suggests that it is the inhomogeneity of antenna Chls in PSI and, in particular, the gross distribution of excitation energies that influences the 1C3PEPS data. We require a more sensitive probe of the exact distribution of excitation energies and coupling strengths within PSI, a method that can measure the evolution of the excitation. As discussed in the Introduction, 2C3PEPS is such a method, as it accesses the time-dependent conditional probability of the system interacting with light at frequency ω_2 given that it was initially excited with frequency ω_1. We will see in the next section that 2C3PEPS is a much more sensitive probe of the energy transfer pathways and, therefore, both the diagonal and off-diagonal elements of the molecular Hamiltonian.

Two-Color Photon Echo Peak Shift. Two-color four-wave mixing experiments were performed with the first two pulses centered at 675 nm (fwhm = 10 nm) and the third pulse centered at 703 nm (fwhm = 14 nm), as shown in Figure 6. The pulses are close to transform-limited with pulse durations of ∼80 fs.

2C3PEPS data, with a probe wavelength of 703 nm, are presented in Figure 7. The type I (echo) and type II (FID) peak shifts have a large initial value, similar to that seen in 1C3PEPS, indicating weak coupling to the bath. The peak shifts decay to

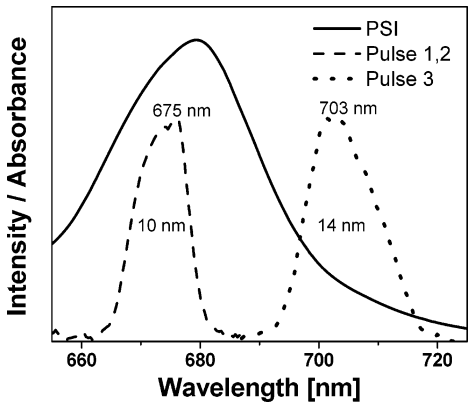

Figure 6. Absorption spectrum of the Q_y band of PSI (solid line) and the laser spectra of the pulses (dashed and dotted lines) employed for the two-color photon echo experiment.

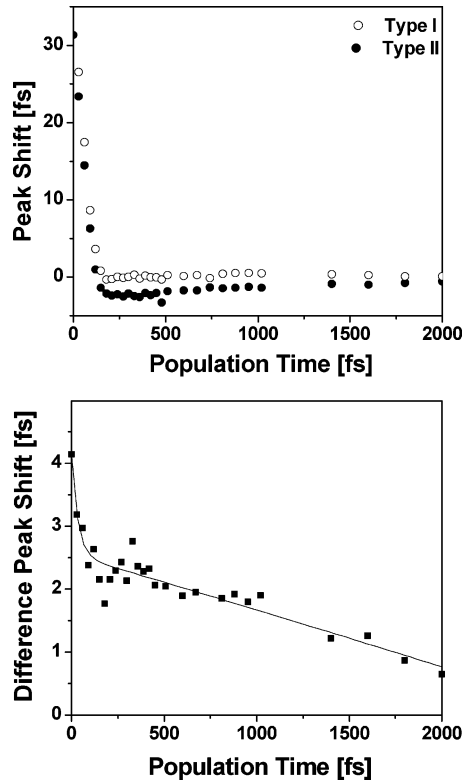

Figure 7. Two-color photon echo peak shift data taken with the 675−675−703 nm pulse combination. The type I and type II peak shifts (top) and the DPS (bottom) are shown. Differential scattering most likely caused the two outlying data points in the peak shift. These points have been removed in the lower figure and in subsequent analysis of the DPS.

almost zero by 200 fs. After 200 fs, the type I peak shift remains relatively constant, while the type II peak shift slightly increases. The DPS is initially ∼4 fs and decays steadily with increasing population time. Unlike previous 2C3PEPS studies,[33,34] the type I and II peak shifts are not symmetric about time zero at longer population times. We propose this to be due to energy transfer.

As explained by Cho and co-workers,[35,45] 2C3PEPS directly accesses the magnitude of the fluctuating transition frequencies cross-correlation function, $\langle \delta\Omega_j \delta\Omega_k \rangle$, where $\delta\Omega_i$ is the energetic fluctuation of the ith exciton state.[35] In the high-temperature limit, $\langle \delta\Omega_j \delta\Omega_k \rangle$ is linearly proportional to the spatial overlap between the two exciton probability densities.[35] Previous 2C3PEPS experiments performed on laser dyes and a coupled dimer system exhibited a zero initial value for the DPS.[33,34] This is not the case in PSI (Figure 7) where instantaneous correlation

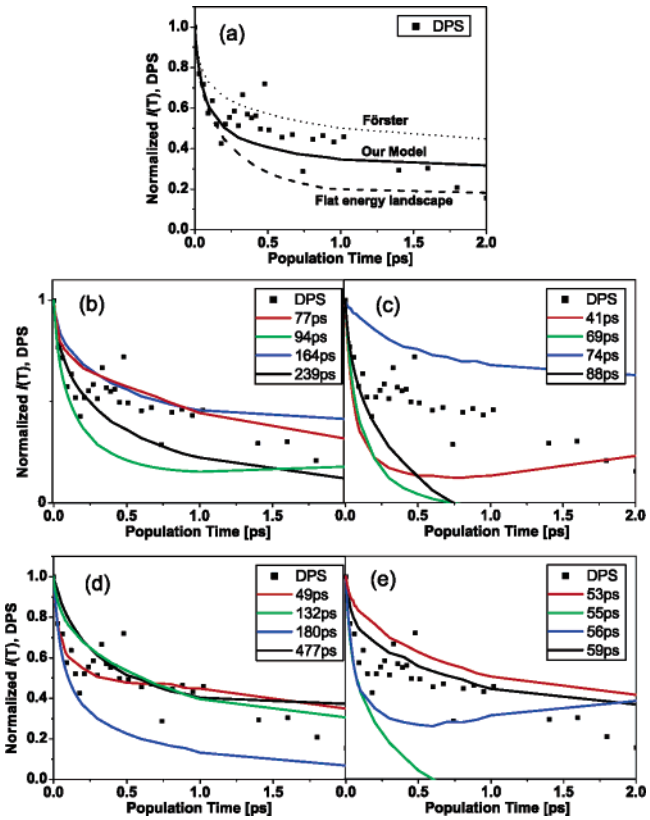

Figure 8. Calculated rephasing capability of PSI, $I(T)$, compared with the DPS for the 675−675−703 nm pulse combination. (a) $I(T)$ computed for the Hamiltonian developed in Chapter 2, using modified Redfield/Förster theory (solid line), Förster theory (dotted line), and using a flat energy landscape within modified Redfield/Förster theory (dashed line). (b) The rephasing capability of PSI computed for various permutations of the site energies, holding the site energy of Chl EC-A1 constant. (c) The same as (b), except the calculated energies of the RC and linker Chls are fixed, and only the energies of the antenna Chls are permuted. (d) The same as (b), except the orientations, and not the energies, are permuted. (e) The same as (c), except the orientation, and not the energies, are permuted. Trapping times for the permuted configurations are shown in the various legends.

exists between absorption at 675 and 703 nm, indicating large spatial overlap between the excitons with transition frequencies initially pumped at 675 nm and those probed at 703 nm.

The DPS can be simulated by calculating the inhomogeneous rephasing capability, $I(T)$, using the Hamiltonian for PSI constructed by Damjanovic et al.[19] and implementing modified Redfield/Förster theory, as in Yang et al.[40] The result is a biexponential curve that fits the data quite well (Figure 8). Under Förster theory, $I(T)$ decays slower than our experimental data. If we use a flat energy landscape, maintaining the computed coupling strengths and allowing for static disorder by using a distribution of Chl site energies (with the width equal to the inhomogeneous width of the PSI absorption spectrum), the calculated $I(T)$ decays much faster, indicating weaker correlation between the excited donor and the probed acceptor Chls.

We tested the sensitivity of the $I(T)$ to the original Hamiltonian constructed previously[19] by randomly shuffling the site energies or the orientations and recalculating the $I(T)$. The $I(T)$ of four sets of configurations for PSI were computed as follows: shuffling all the Chl site energies except the excitation energy of the epimer (Chl EC-A1); permuting the site energies of the antenna Chls, while maintaining the site energies for the six RC and two linker Chls at their calculated values; varying the orientations of all the Chls except for the epimer; and shuffling the orientations of the antenna Chls but not the RC and linker Chls. When permuting the site energies, the coupling parameters obtained by Damjanovic et al.[19] were used, whereas when the orientations were permuted, the coupling constants were recalculated using the dipole−dipole approximation. Figure 8 shows the resulting $I(T)$s for the four sets of configurations. The trapping times associated with the various configurations illustrated range from 40 to 500 ps compared to an experimental trapping time of 36 ps. Unlike the trapping time or the absorption spectrum, the 2C3PEPS $I(T)$ is very sensitive to the energy landscape and the pathways of energy transport, demonstrated by the drastically changing decay of $I(T)$.

Conclusions

In comparing experimental data to theoretical models in a system as complex as PSI, one is immediately confronted with the small numbers of parameters accessible from conventional time-resolved spectroscopic measurements with which to calibrate the success of the theory. From transient absorption and time-resolved fluorescence studies, the overall trapping time and exponential decay (and in some cases, rise) components can be obtained. The trapping time is a key parameter, but many different 96 × 96 rate matrixes can result in the same trapping time. Similarly, the time scales obtained from multiexponential fits relate to complex averages of the underlying microscopic behavior, and while our previous success[40] in matching the experimental time scales (and in rationalizing why such fits do roughly characterize the key time scales in the rate matrix) is encouraging, such agreement is insufficient to verify the details of the calculation. In particular, how well the spatial arrangement of the calculated energies is captured in the calculations of ref 22 cannot be assessed from conventional measurements.

In the present paper, we have explored the extent to which more complex experimental techniques such as the one- and two-color photon echo peak shift experiments can provide more stringent tests of our ability to calculate the nature of the electronic states, the energy landscape, and the energy flow within PSI. Both of the experiments and the modeling approaches represent first approaches to such a complex system, yet the consistent picture of the one-color data offered by the two calculation methods suggests that the essential aspects of the energy transfer dynamics have been captured.

Our one-color data clearly show that the electronic states assessed at 715 nm are quite different from those at short wavelengths. Our results are consistent with the expectation that such a large red-shift arises from strong excitonic coupling, and the consequent increase in electron−phonon coupling arising from charge-transfer contributions to the excited state wave function. The wavelength-dependent and bandwidth-dependent one-color data provide details on the most likely energy transfer partners at different locations in the energy distribution. In systems with fewer pigments (e.g., LHC II), it is likely that such measurements could provide detailed information on the coupling of spatial and energetic dynamics.

Although limited to a single pair of wavelengths in this study, the new technique of 2C3PEPS and, in particular, the DPS shows considerable promise for characterizing energy landscapes and energy flows. First, the DPS is quite sensitive to the method of calculation of the energy transfer rates. In our combined experimental and theoretical study of the FMO complex, using two-dimensional electronic spectroscopy,[35,46] we demonstrated that delocalized excitonic states allow larger energy jumps than is predicted assuming Förster transfer between localized excitations on the same molecules. This is most likely the cause of

the faster decay of the DPS in Figure 8a when calculated using modified Redfield/Förster theory[40] compared to when pure Förster theory is used. Second, the DPS is very sensitive to energy locations and transition moment orientations of the 96 Chl molecules, even though the overall trapping time may not be. Figure 8e shows a particularly striking example of this, where the trapping times vary by only 6 ps, but the DPS curves vary widely. Given this sensitivity, the agreement between the calculated DPS using the model of ref 22 and the experimental DPS is very encouraging. An important test of these conclusions would be to carry out similar experiments on *Synechocystis*, which contains fewer red Chls than *Synechococcus*. Further, in silico studies would also be valuable.

A striking feature of the experimental DPS and, therefore, of the type I and type II peak shift curves from which it is constructed is the lack of a rising component in the difference peak shift. For systems lacking energy transfer, unless the probe wavelength is in resonance with a strongly coupled vibrational transition, the DPS begins near zero, rises to a maximum, and decays[32−34,47] as Chl in PSI does not have strongly enough coupled vibrational modes to produce a one-color-like two-color signal[47] at this wavelength. In PSI, the DPS obtained with 675−675−705 nm pulses begins with a finite value and decays. This strongly suggests that a large spatial overlap exists between excitons absorbing in the bulk and those absorbing at 705 nm and/or there are unresolved ultrafast energy transfer steps between the 675 and the 705 nm Chls. Ultrafast energy transfer is, of course, expected between the upper and the lower members of an excitonically coupled dimer, for example, so that the two effects are not likely to be independent. Similarly, the asymmetric behavior of the type I and type II peak shifts at larger times, with respect to zero peak shift, most likely results from the energy transfer dynamics.

The good agreement of both one- and two-color peakshift data with calculations based on the model of ref 22 encourage us to reiterate and expand on the conclusions reached on energy transfer and trapping in PSI, previously based entirely on the theoretical rate matrix[23,40] and the kinetic domain model constructed from it.[48] A two-dimensional projection of the structure of PSI suggests that the RC Chls are isolated from the antenna Chls in much the same way as in the RC/LH1 complex of purple bacteria. However, this is not so. If an excitation arrives on a RC Chl, it is more likely the excitation returns to the antenna than gets trapped at P700. Indeed, the kinetic domain model shows that 47% of the overall trapping time arises from two domains associated with the RC Chls.[48] In other words, the trapping is dominated by entropic considerations arising from the large number of Chls that can accept "back transfer" from the RC Chls, rather than enthalpic effects arising from an energy funnel. The fact that the calculated energy landscape of PSI is consistent with the landscape-sensitive 2C3PEPS measurements strengthens the confidence we have in this picture of PSI function. PSI and the purple bacterial RC1/LH1 complex efficiently solve the same problem in two different ways—the high spatial connectivity of PSI allows for an energetically disordered antenna and obviates the need for an energy funnel.

In summary, the sensitivity of 3PEPS, and especially the two-color version, 2C3PEPS, to the precise distribution of energies and couplings in energy transfer networks illuminates aspects of these systems that were previously inaccessible to experiment. We hope the 2C3PEPS technique will find wide application as the ability to generate synchronized multicolor ultrashort pulses becomes routine.

Acknowledgment. This work used resources provided by the National Energy Research Scientific Computing Center and was supported by the Director, Office of Science, Office of Basic Energy Sciences, Chemical Sciences Division, of the U.S. Department of Energy under Contract No. DE-AC03-76SF00098. J.S. thanks the German Academic Exchange Service (DAAD) for a postdoctoral fellowship. We thank Minhaeng Cho, Mino Yang, Bradley Prall, Andrei Pisliakov, and Tomas Mancal for useful discussions and Ingo Grotjohann and Hongqi Yu for the preparation and crystallization of our samples. P.F. supported by NSF grant MCB-0417142.

References and Notes

(1) Jordan, P.; Fromme, P.; Witt, H. T.; Klukas, O.; Saenger, W.; Krauss, N. *Nature* **2001**, *411*, 909.
(2) Fromme, P.; Witt, H. T. *Biochim. Biophys. Acta* **1998**, *1365*, 175.
(3) Ben-Shem, A.; Frolow, F.; Nelson, N. *FEBS Lett.* **2004**, *564*, 274.
(4) Byrdin, M.; Rimke, I.; Schlodder, E.; Stehlik, D.; Roelofs, T. A. *Biophys. J.* **2000**, *79*, 992.
(5) Gobets, B.; van Grondelle, R. *Biochim. Biophys. Acta* **2001**, *1507*, 80.
(6) Holzwarth, A. R.; Schatz, G.; Brock, H.; Bittersmann, E. *Biophys. J.* **1993**, *64*, 1813.
(7) Savikhin, S.; Xu, W.; Chitnis, P. R.; Struve, W. S. *Biophys. J.* **2000**, *79*, 1573.
(8) Savikhin, S.; Xu, W.; Soukoulis, V.; Chitnis, P. R.; Struve, W. S. *Biophys. J.* **1999**, *76*, 3278.
(9) Kennis, J. T. M.; Gobets, B.; van Stokkum, I. H. M.; Dekker, J.; van Grondelle, R.; Fleming, G. R. *J. Phys. Chem. B* **2001**, *105*, 4485.
(10) Melkozernov, A. N.; Lin, S.; Blankenship, R. E. *Biochemistry* **2000**, *39*, 1489.
(11) Melkozernov, A. N.; Lin, S.; Blankenship, R. E.; Valkunas, L. *Biophys. J.* **2001**, *81*, 1144.
(12) Gobets, B.; van Amerongen, H.; Monshouwer, R.; Kruip, J.; Roegner, M.; van Grondelle, R.; Dekker, J. *Biochim. Biophys. Acta* **1994**, *1188*, 75.
(13) Gobets, B.; Dekker, J. P.; van Grondelle, R. Transfer-to-Trap Limited Model of Energy Transfer in Photosystem I. In *Photosynthesis: Mechanisms and Effects*; Garab, G., Ed.; Kluwer Academic Publishers: Dordrecht, Germany, 1998; p 503.
(14) Palsson, L. O.; Dekker, J. P.; Schlodder, E.; Monshouwer, R.; van Grondelle, R. *Photosynth. Res.* **1996**, *48*, 239.
(15) Palsson, L. O.; Flemming, C.; Gobets, B.; van Grondelle, R.; Dekker, J. P.; Schlodder, E. *Biophys. J.* **1998**, *74*, 2611.
(16) Gobets, B.; van Stokkum, I. H. M.; van Mourik, F.; Dekker, J. P.; van Grondelle, R. *Biophys. J.* **2003**, *85*, 3883.
(17) Gobets, B.; van Stokkum, I. H. M.; Rogner, M.; Kruip, J.; Schlodder, E.; Karapetyan, N. V.; Dekker, J. P.; van Grondelle, R. *Biophys. J.* **2001**, *81*, 407.
(18) Byrdin, M.; Jordan, P.; Krauss, N.; Fromme, P.; Stehlik, D.; Schlodder, E. *Biophys. J.* **2002**, *83*, 433.
(19) Damjanovic, A.; Vaswani, H. M.; Fromme, P.; Fleming, G. R. *J. Phys. Chem. B* **2002**, *106*, 10251.
(20) Sener, M. K.; Lu, D. Y.; Ritz, T.; Park, S.; Fromme, P.; Schulten, K. *J. Phys. Chem. B* **2002**, *106*, 7948.
(21) Sener, M. K.; Park, S.; Lu, D. Y.; Damjanovic, A.; Ritz, T.; Fromme, P.; Schulten, K. *J. Chem. Phys.* **2004**, *120*, 11183.
(22) Fleming, G. R.; Yang, M.; Agarwal, R.; Prall, B. S.; Kaufman, L. J.; Neuwahl, F. V. R. *Bull. Korean Chem. Soc.* **2003**, *24*, 1081.
(23) Vaswani, H. M.; Yang, M.; Damjanovic, A.; Fleming, G. R. The Mechanism of Energy Transfer and Trapping in Photosystem I. In *Ultrafast Molecular Events in Chemistry and Biology*; Martin, M. M., Hynes, J. T., Eds.; Elsevier: New York, 2004; Vol. 6; p 401.
(24) Yang, M.; Fleming, G. R. *J. Chem. Phys.* **2000**, *113*, 2823.
(25) Yang, M.; Fleming, G. R. *J. Chem. Phys.* **1999**, *111*, 27.
(26) Agarwal, R.; Rizvi, A. H.; Prall, B. S.; Olsen, J. D.; Hunter, C. N.; Fleming, G. R. *J. Phys. Chem. A.* **2002**, *106*, 7573.
(27) Agarwal, R.; Yang, M.; Xu, Q.-H.; Fleming, G. R. *J. Phys. Chem. B* **2001**, *105*, 1887.
(28) Jimenez, R.; van Mourik, F.; Yu, J. Y.; Fleming, G. R. *J. Phys. Chem. B* **1997**, *101*, 7350.
(29) Yu, J.-Y.; Nagasawa, Y.; van Grondelle, R.; Fleming, G. R. *Chem. Phys. Lett.* **1997**, *280*, 404.
(30) Cho, M.; Yu, J.-Y.; Joo, T.; Nagasawa, Y.; Passino, S. A.; Fleming, G. R. *J. Phys. Chem.* **1996**, *100*, 11944.
(31) Yang, M.; Fleming, G. R. *J. Chem. Phys.* **1999**, *110*, 2983.
(32) Prall, B. S. Femtosecond degenerate four-wave mixing: the two-color photon echo peak shift. Ph.D. Thesis, University of California, Berkeley, 2005.

(33) Prall, B. S.; Parkinson, D. Y.; Yang, M.; Ishikawa, N.; Fleming, G. R. *J. Chem. Phys.* **2004**, *120*, 2537.
(34) Agarwal, R.; Prall, B. S.; Rizvi, A. H.; Yang, M.; Fleming, G. R. *J. Chem. Phys.* **2002**, *116*, 6243.
(35) Cho, M.; Vaswani, H. M.; Brixner, T.; Stenger, J.; Fleming, G. R. *J. Phys. Chem. B* **2005**, *109*, 10542.
(36) Joo, T. H.; Jia, Y. W.; Yu, J. Y.; Lang, M. J.; Fleming, G. R. *J. Chem. Phys.* **1996**, *104*, 6089.
(37) de Boeij, W. P.; Pshenichnikov, M. S.; Wiersma, D. A. *Annu. Rev. Phys. Chem.* **1998**, *49*, 99.
(38) de Boeij, W. P.; Pshenichnikov, M. S.; Wiersma, D. A. *J. Phys. Chem.* **1996**, *100*, 11806.
(39) Joo, T.; Jia, Y. W.; Fleming, G. R. *Opt. Lett.* **1995**, *20*, 389.
(40) Yang, M.; Damjanovic, A.; Vaswani, H. M.; Fleming, G. R. *Biophys. J.* **2003**, *85*, 140.
(41) Gillie, J. K.; Small, G. J.; Golbeck, J. H. *J. Phys. Chem.* **1989**, *93*, 1620.
(42) Zucchelli, G.; Jennings, R. C.; Garlaschi, F. M.; Cinque, G.; Bassi, R.; Cremonesi, O. *Biophys. J.* **2002**, *82*, 378.
(43) Agarwal, R.; Krueger, B. P.; Scholes, G. D.; Yang, M.; Yom, J.; Mets, L.; Fleming, G. R. *J. Phys. Chem. B* **2000**, *104*, 2908.
(44) Vaswani, H. M. A theoretical and femtosecond spectroscopic investigation of energy transfer in photosynthetic complexes. Ph.D. Thesis, University of California, Berkeley, 2005.
(45) Cho, M.; Fleming, G. R. *J. Chem. Phys.* **2005**, *123*, 114506.
(46) Brixner, T.; Stenger, J.; Vaswani, H. M.; Cho, M.; Blankenship, R. E.; Fleming, G. R. *Nature* **2005**, *343*, 625.
(47) Prall, B. S.; Parkinson, D. Y.; Fleming, G. R. *J. Chem. Phys.* **2005**, *123*, 054515.
(48) Yang, M.; Fleming, G. R. *J. Chem. Phys.* **2003**, *119*, 5614.